Applied Surface Science 255 (2009) 7812–7817

Contents lists available at ScienceDirect

Applied Surface Science

journal homepage: www.elsevier.com/locate/apsusc

Study of interfacial reactions and phase stabilization of mixed Sc, Dy, Hf high-k oxides by attenuated total reflectance infrared spectroscopy

A. Hardy [a,b], C. Adelmann [c], S. Van Elshocht [c], H. Van den Rul [a,b], M.K. Van Bael [a,b,*], S. De Gendt [c,e], M. D'Olieslaeger [b,d], M. Heyns [c,e], J.A. Kittl [c], J. Mullens [a]

[a] Hasselt University, Inorganic and Physical Chemistry – IMO, Diepenbeek, Belgium
[b] IMEC vzw, Division IMOMEC, Diepenbeek, Belgium
[c] IMEC vzw, Heverlee, Belgium
[d] Hasselt University, Institute for Materials Research, Diepenbeek, Belgium
[e] KULeuven, Department of Chemistry, Heverlee, Belgium

ARTICLE INFO

Article history:
Received 19 March 2009
Received in revised form 27 April 2009
Accepted 28 April 2009
Available online 3 May 2009

Keywords:
ATR-FTIR
Hafnia
Scandate
Rare earth
High permittivity

ABSTRACT

Grazing angle attenuated total reflectance Fourier transform infrared spectroscopy is applied to study ultrathin film Hf^{4+}, Sc^{3+} and Dy^{3+}oxides, due to its high surface sensitivity. The (multi)metal oxides studied, are of interest as high-k dielectrics. Important properties affecting the permittivity, such as the amorphous or crystalline phase and interfacial reactions, are characterized.

Dy_2O_3 is prone to silicate formation on SiO_2/Si substrates, which is expressed in $DyScO_3$ as well, but suppressed in $HfDyO_x$. Sc_2O_3, $HfScO_x$ and HfO_2 were found to be stable in contact with SiO_2/Si. Deposition of HfO_2 in between Dy_2O_3 or $DyScO_3$ and SiO_2, prevents silicate formation, showing a buffer-like behavior for the HfO_2.

Doping of HfO_2 with Dy or Sc prevents monoclinic phase crystallization. Instead, a cubic phase is obtained, which allows a higher permittivity of the films. The phase remains stable after anneal at high temperature.

© 2009 Elsevier B.V. All rights reserved.

1. Introduction

Downscaling of CMOS transistors has allowed continuously increasing device speed and improved performance. As a consequence of the miniaturization the gate dielectric, SiO_2, thickness has been decreased strongly. Recently, commercial production has switched to alternative gate dielectric materials with a higher permittivity than SiO_2 ($k = 3.9$), in order to control the leakage current. Due to the higher permittivity, the physical thickness is higher than the effective oxide thickness (EOT), which allows avoiding electron tunneling through the dielectric oxide [1,2].

Hafnium based materials such as amorphous HfO_2 ($k \sim 22$ [3]) and $(Hf,Si)O_2$ mixed compositions have recently received a great deal of attention. The amorphicity or crystalline phase strongly affects the permittivities which are achieved. The thermodynamically stable crystal structure of HfO_2 at room temperature is monoclinic and is characterized by a $k \sim 16$ [4]. Tetragonal and cubic high temperature phases on the other hand show much higher permittivities ($k \sim 70$ and 29 respectively [4]). These phases have been shown to be stabilized by doping HfO_2 with lanthanides [5–8]. Besides Hf based materials, lanthanide scandates are reported to be promising as high-k dielectrics, due to their high permittivity (>20) and crystallization resistance up to high temperatures, which is explained by silicate formation [6,9,10].

Independent of the high-k material, MOS device performance is always affected by reactions at the interface with the SiO_x/Si substrate, such as silicate formation or regrowth of interfacial SiO_x. These interfacial layers can be characterized by a lower permittivity and thus lead to undesirable increase of the EOT of the stack. However, often a very thin starting SiO_x is required to obtain layer nucleation e.g. in atomic layer deposition [11–13], and therefore cannot be avoided. The control of its thickness during further processing then remains crucial [1].

The ultralow thickness of the high-k layers (<10 nm), necessitates the use of highly sensitive characterization techniques, such as grazing incidence X-ray diffraction (XRD), cross section transmission electron microscopy (TEM), TOF-SIMS (time of flight secondary ion mass spectrometry), or XPS (X-ray photoelectron spectroscopy). FTIR (Fourier transform infrared

* Corresponding author at: Hasselt University, Inorganic and Physical Chemistry, Agoralaan building D, B-3590 Diepenbeek, Belgium. Tel.: +32 11 26 83 07; fax: +32 11 26 83 01.
E-mail addresses: an.hardy@uhasselt.be (A. Hardy), marlies.vanbael@uhasselt.be (M.K. Van Bael).

0169-4332/$ – see front matter © 2009 Elsevier B.V. All rights reserved.
doi:10.1016/j.apsusc.2009.04.184

spectroscopy) allows the detection of metal oxide as well as silicate vibrations. Normal transmission measurements are insufficiently sensitive, but the surface sensitivity can be greatly enhanced in attenuated total reflectance (ATR) [14]. The sensitivity enhancement depends on the angle of incidence, the thickness of the air gap and the dielectric constants of the ATR crystal and the film's substrate [15,16].

Here, we apply grazing angle attenuated total reflectance Fourier transform infrared (GATR-FTIR) to several high-*k* films of recent interest, Hf, Dy and Sc oxides, which were deposited by atomic vapour deposition (AVD) or atomic layer deposition (ALD) for high quality film growth with atomic precision. The results contribute to the explanation and understanding of the dielectric properties, demonstrating the potential of GATR-FTIR in high-*k* characterization.

2. Material and methods

All the high-*k* films were grown by AVD (Aixtron Tricent^{TM} reactor) on Si (1 0 0) wafers as described elsewhere [6,9,17,18], with 550 °C susceptor temperature, unless indicated otherwise. Precursors used were tris(6-ethyl-2,2-dimethyl-3,5-decanedionato)dysprosium [$Dy(EDMDD)_3$], tris(6-ethyl-2,2-dimethyl-3,5-decanedionato) scandium [$Sc(EDMDD)_3$], and bis(*tert*-butoxide) bis(methoxymethyl propanoxide) hafnium $Hf(O^tBu)_2$ (mmp)$_2$ combined with molecular O_2. SiO_2 starting oxide was obtained with a thickness of 1.1 nm by chemical oxidation (H_2O/O_3), while thicker SiO_2 was obtained by rapid thermal oxidation. Film thicknesses were determined by X-ray reflectivity. The compositions of the films are determined by X-ray photoelectron spectroscopy ($HfDyO_x$, $HfScO_x$) and Rutherford backscattering spectroscopy ($DyScO_3$). The doped HfO_2 films contain 10% Dy or Sc (90% Hf) and the $DyScO_3$ consists of 50% Dy and 50% Sc unless specified otherwise (percentages ignoring O, e.g. Dy/Dy + Hf). Post deposition anneals were carried out at 1000 °C in N_2 or O_2 for 60 s.

Sample preparation for grazing angle attenuated total reflectance Fourier transform infrared measurement consists of cleaving square pieces (2 cm × 2 cm to 3 cm × 3 cm) from the wafers. GATR-FTIR spectroscopy was carried out by means of a 65° single reflection Ge-ATR (supplied by Harrick), placed in the sample compartment of an FTIR spectrometer (Bruker, Vertex 70). The compartment and the GATR-cell were flushed with dried air and N_2 respectively. Intimate contact between the sample and the Ge crystal is obtained by applying 56 oz in.$^{-1}$ of pressure. Spectra were referenced against the clean Ge crystal and obtained with a spectral resolution of 4 cm^{-1}, in a spectral range from 4000 to 600 cm^{-1}. For the spectra, the ATR signal = (absorbance × wavenumber)/1000 is shown. Since the penetration depth is inversely proportional to the wavenumber this normalizes the spectra to a constant penetration depth. In between the samples, blank 1.2 nm SiO_x/Si samples were measured, showing no changes in the Ge crystal's state, such as scratches, which would affect the spectra and interfere with the comparison of different samples.

3. Results and discussion

3.1. Monometal oxides

3.1.1. Phase identification of hafnium oxide

The permittivity of the HfO_2 layers studied here was determined to be 16, as published elsewhere [6]. This value can be characteristic either for amorphous or monoclinic HfO_2.

HfO_2 layers with thicknesses of 3, 8 and 18 nm on 1.1 nm SiO_2/Si have been characterized and their spectra are compared to a blank SiO_x/Si substrate (Fig. 1a). Band assignments and interpretations are as follows. At 1240 and 1065 cm^{-1} the longitudinal (LO) and

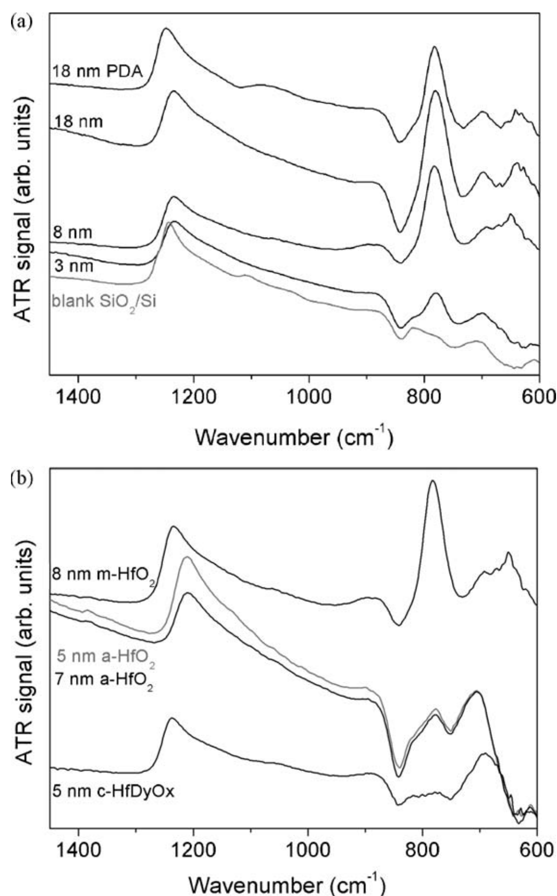

Fig. 1. GATR-FTIR spectra of (a) monoclinic HfO_2 as function of thickness, (b) comparison of different phases of (stabilized) hafnia in films of comparable thickness (a: amorphous, c: cubic, m: monoclinic).

transverse optic (TO) band of SiO_2 are found [15]. At 1100 cm^{-1} Hf–O–Si vibrations would be expected [19], but comparison with the blank substrates shows that any intensity in this area is due to the SiO_2 from the substrate [20]. At 900 cm^{-1} both the blank substrate and the HfO_2 films show slightly increased intensity, which might be ascribed to Si–OH [21]. The band at 780 cm^{-1} can be ascribed to the monoclinic crystal phase of HfO_2, which forms a doublet together with the weaker feature at 690–700 cm^{-1}. Theory predicts this doublet to be situated at 780/694 cm^{-1} and 683/634 cm^{-1} [4], and it has been ascribed experimentally to peaks at 760 cm^{-1} [7] or 752 and 635 cm^{-1}[16,22,23]. Based on the presence of this vibration around 780 cm^{-1} in the spectra of HfO_2 films of all thicknesses studied, it can be concluded that all of these films contain monoclinic HfO_2.

Post deposition anneal in O_2 (PDA, 1000 °C) does not affect the HfO_2 band position and relative intensities. There is no evidence for Hf–O–Si vibrations around 1100 cm^{-1}. It can be concluded that the anneal does not affect the HfO_2 phase present, nor leads to interfacial silicate formation.

Theoretically, it is impossible to observe the bands for the higher-*k* cubic phase of HfO_2, situated at 286 cm^{-1}, in the measurable range of Ge-ATR [4]. Nonetheless, a single band at 695 cm^{-1}, in absence of a feature at 780 cm^{-1}, has been ascribed to cubic HfO_2, because electron diffraction showed the presence of this phase in the samples [7]. The authors however did not demonstrate the absence of a portion amorphous phase, which is also reported to show a single band of similar shape in this wavenumber region of 690 cm^{-1} [3,16,24]. The presence or absence of a shoulder to the high wavenumber side of this band,

is regarded as indicative of amorphous and cubic HfO_2 respectively [25]. Since literature reports appear contradictive as far as distinction of cubic and amorphous HfO_2 is concerned, we studied XRD-amorphous HfO_2 films, deposited by ALD at 250 °C using $HfCl_4$ and H_2O [26], by GATR-FTIR as well (Fig. 1b). The comparison shows a clear distinction between the amorphous, cubic and monoclinic phase. Monoclinic HfO_2 is distinguished by a strong band ~780 cm^{-1} and a much less intense vibration around 700 cm^{-1}. $HfDyO_x$ shows a feature around 690 cm^{-1} and very low intensity around 780 cm^{-1}. Due to the peak half width in XRD being of the order of or larger than the peak splittings expected, there is no evidence for tetragonal phase, and therefore the $HfDyO_x$ layers were assigned as cubic phase. Amorphous HfO_2 is characterized by a vibration around 780 and 700 cm^{-1} as well, but the relative intensities of the bands are clearly different from c-HfO_2 and m-HfO_2. Note that by comparison of similar layer thicknesses, optical effects as a function of thickness are cancelled out from the discussion.

In conclusion, the GATR-FTIR results shown here, allow to ascribe the experimentally observed permittivity of 16 [6] to the monoclinic crystal phase of these HfO_2 layers. This is in accordance with X-ray diffraction patterns reported in Ref. [6]. In literature [24], ultrathin films are reported to remain amorphous, but here a 3 nm thick film was crystalline, monoclinic phase. The GATR-FTIR is shown to be more sensitive to monoclinic HfO_2 than deep-UV micro-Raman spectrometry, where it was not distinguished from the noise in a 3 nm thick HfO_2 layer.

3.1.2. Interfacial reactions of dysprosium and scandium oxide

10 nm thick Dy_2O_3 monometal oxide films were studied for comparison with $HfDyO_x$ and $DyScO_3$. The spectra of dysprosium oxide grown on 1.1 nm SiO_2, 20 nm SiO_2 and 12 nm HfO_2 are shown in Fig. 2, and are compared to the respective blank substrates. For the thin SiO_x substrate it is clear that the SiO_x characteristic band at 1240 cm^{-1} disappears from the spectrum and a strong, new band occurs with a peak maximum at 1017 cm^{-1}. The latter band is ascribed to Si–O–Dy vibrations. Bond formation with Dy, which is heavier than Si, shifts the band to lower frequencies compared to the Si–O–Si band [27]. This demonstrates strong silicate formation, which apparently consumes the SiO_2 entirely. Typical Dy–O vibrations are not detected as they are situated below 600 cm^{-1} e.g. 550 or 555 cm^{-1} with a broad shoulder at 580 cm^{-1}, is expected [28–31]. Chemical instability of Dy_2O_3 by reaction with H_2O or CO_2 from the ambient probably did not occur, as (bi)carbonate (3727, 3711, 1661, 1634 cm^{-1} [32]) and hydroxide bands (3600 cm^{-1} [33]) were not detected in the spectra. This can be related to a stronger stability of Dy_2O_3 against these reactions compared to other Ln_2O_3 [34]. Deposition of 10 nm Dy_2O_3 on 20 nm RTO SiO_2 clearly shows a very strong band in the same wavenumber region as the Si–O–Dy band for the Dy_2O_3/1.1 nm SiO_2 film. For the blank 10 nm SiO_2 substrate, the intensity around 1050 cm^{-1} is strong as well, and the band shape and position of SiO_2 is strongly dependent on the SiO_2 thickness due to optical effects of interference [15]. However, the intensity of the band at ~1050 cm^{-1} is relatively much stronger compared to the LO SiO_2 band at 1225 cm^{-1} for the Dy_2O_3 film than for the blank 10 nm SiO_2 substrate. This suggests that silicate formation occurs in the Dy_2O_3/20 nm SiO_2 film as well and is more intense than for 1.1 nm SiO_2. 10 nm Dy_2O_3 films deposited on 12 nm HfO_2 on the other hand, showed SiO_2 LO and TO bands similar to a blank substrate and no evidence for Dy–O–Si vibrations. The monoclinic phase of HfO_2 is demonstrated by its characteristic vibration at 780 cm^{-1}. It can be concluded that HfO_2 acts as an efficient barrier, preventing silicate formation of Dy_2O_3.

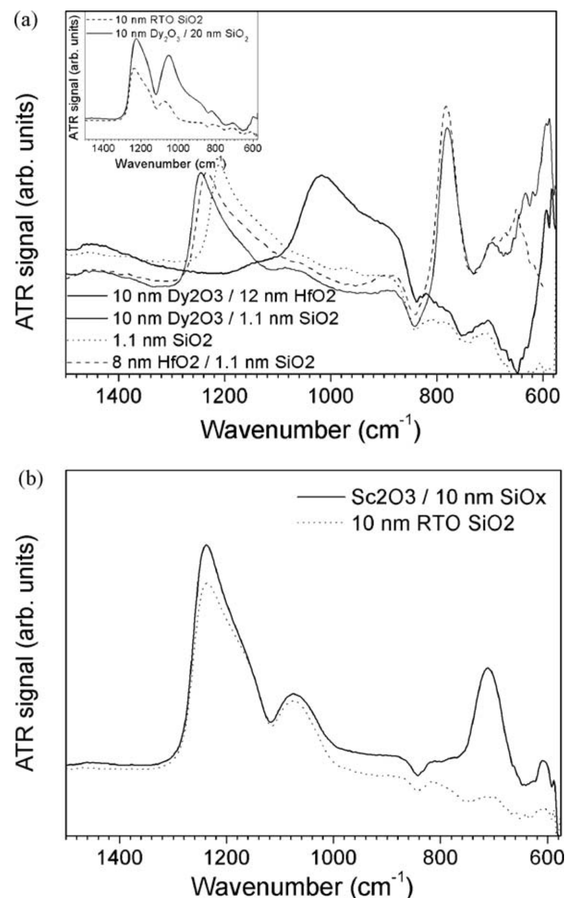

Fig. 2. (a) 10 nm Dy_2O_3 on different substrates as indicated, (b) 10 nm Sc_2O_3/10 nm SiO_2.

In contrast with Dy_2O_3, a 10 nm Sc_2O_3 film on 10 nm RTO SiO_x did not show any silicate formation, as the relative intensity of SiO_2 TO and LO was identical to the blank substrate. This is in accordance with the reported thermodynamic stability of Sc_2O_3 in contact with SiO_2 [35]. Vibration bands are observed at 711 and 609 cm^{-1}, which should be ascribed to Sc_2O_3. Comparison with literature on the other hand, shows expected bands at 625 or 635 cm^{-1} [28,29] for C-type oxide [36]. The discrepancy is neither related to an amorphous nature of the layer, as its crystallinity was evidenced by XTEM (not shown), nor to a difference in crystal structure as Sc_2O_3 has no known polymorphs, only the cubic bixbyite phase [37].

3.2. Multimetal oxides

3.2.1. Phase identification and interfacial reactions of dysprosium and scandium doped hafnia

Doping hafnia with lanthanides has been reported to stabilize the cubic phase in HfO_2, leading to higher permittivities and prolonging its applicability for commercial purposes [6]. Here, the phase stabilization of cubic hafnia by doping with Dy and Sc is studied by GATR-FTIR.

In Fig. 3 spectra of as-deposited $HfDyO_x$ films with thicknesses of 3, 5 and 18 nm are shown. Spectra are shifted along the ordinate for clarity. As the band assignments are the same as for hafnia itself, it is clear from Fig. 3 that the doping with Dy has prevented the crystallization of monoclinic hafnia, indicated by the absence of a vibration band around 780 cm^{-1}. Instead, either an amorphous or a cubic phase has been formed, as indicated by the band around 695 cm^{-1}, and the latter was confirmed by X-ray diffraction as

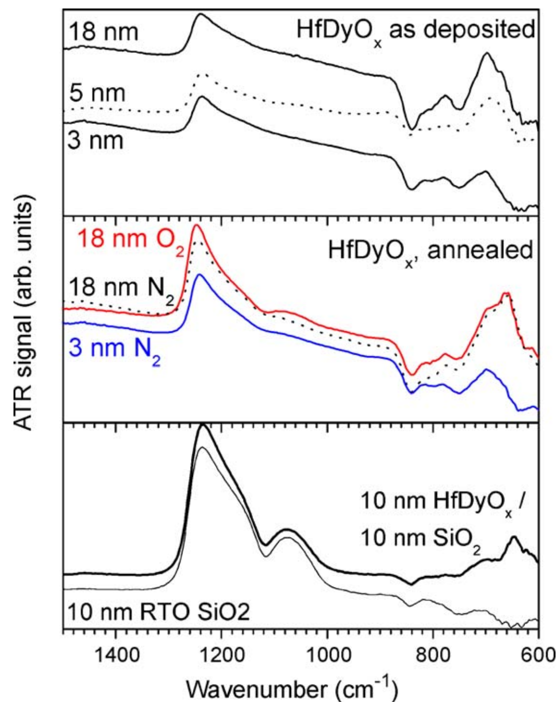

Fig. 3. GATR-FTIR spectra of $HfDyO_x$ films, with thickness, deposited on substrates, with or without anneal as indicated.

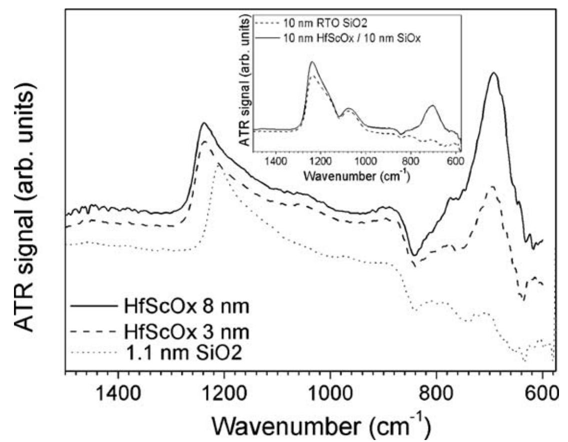

Fig. 4. GATR-FTIR spectra of $HfScO_x$ films with thickness and substrates as indicated.

reported earlier [6]. The cubic phase is stable during anneal in oxygen or nitrogen without transforming into the monoclinic phase. There is no evidence for silicate formation: in the region between 1250 and 1000 cm^{-1} the spectrum does not differ significantly from the blank substrate, both in the as-deposited films and after anneal. This is a large contrast with the results for Dy_2O_3 and $DyScO_3$ (see further), both being characterized by strong silicate formation and contrasts with expectations for lanthanide containing oxides. Very recently, the high efficiency of Hf for suppression of silicate formation of Dy_2O_3 was also shown by investigation of silicate formation through ellipsometric thickness determinations, since only above 75% Dy content the silicate formation became pronounced [35]. Application of a thicker SiO_2 starting surface for $HfDyO_x$ growth, did not lead to silicate formation in $HfDyO_x$ either, which is clear by comparison of 10 nm $HfDyO_x$/10 nm SiO_2 with a blank 10 nm SiO_2/Si substrate. Like for the 1.1 nm SiO_2 starting surface, a stabilized cubic phase $HfDyO_x$ is formed on 10 nm RTO SiO_2 as well. Annealing $HfDyO_x$ 3 nm thick in N_2 or 18 nm thick in N_2 or O_2 did not lead to significant changes as far as the phase or the absence of silicate is concerned. Since it can be expected that the thick films are completely crystallized after anneal, this further strengthens ascribing the band at 695 cm^{-1} to the cubic phase, together with the increased *k*-value and XRD pattern. The regrowth of the SiO_2 interfacial layer is indicated by the increased intensity of the SiO_2 LO and TO bands after anneal in O_2.

$HfScO_x$ films of 3 and 8 nm grown on 1.1 nm SiO_2 are characterized as cubic phase as well, based on the absence of the typical vibration band around 780 cm^{-1} (Fig. 4). This is in agreement with X-ray diffraction [6]. Thicker films show an increased signal intensity, but the peak shape and position are constant, therefore the phase is stable independent of the film thickness in this range. Furthermore, there is no evidence for silicate formation, as the SiO_2 LO and TO region are similar to a blank substrate. 10 nm $HfScO_x$ grown on 10 nm SiO_x substrates have the same crystal structure, and are resistant to silicate formation as well.

Due to the stabilization of the cubic phase, the permittivity rose from 16 for pure HfO_2 to 32 for Dy and Sc doped HfO_2 [6] in accordance with Refs. [5,8].

3.2.2. Interfacial reactions of dysprosium scandate

10 nm $DyScO_3$ layers were deposited on 1.1 nm SiO_x and 12 nm HfO_2 substrates. The GATR-FTIR spectra (Fig. 5) show a strong, broad band with a maximum at 990 cm^{-1} for the SiO_x based film. This band gives evidence for the formation of Si–O–Ln silicate bonds. The band's shape and position resemble those of an analogous Dy_2O_3 film (Fig. 2). However, $DyScO_3$ still has a larger shoulder at 1160 cm^{-1}, indicating less interaction with SiO_2 than for Dy_2O_3. The larger Ln^{3+} radius of Dy^{3+} compared to Sc^{3+} allows increased diffusion of Si from the substrate into Dy_2O_3 than Sc_2O_3 or $DyScO_3$, leading to more Si–O–Ln bond formation [27]. Even though Ono et al. did not study Sc^{3+}, it is possible that the trend continues for Sc^{3+} as well.

10 nm $DyScO_3$ was grown on 12 nm HfO_2 as well (Fig. 5). The presence of monoclinic HfO_2 is confirmed by the vibration at 780 cm^{-1}. Here, no evidence for silicate formation in the wavenumber region around 1050 cm^{-1} is found, indicating that HfO_2 is acting as a buffer for Dy silicate formation, similar as for Dy_2O_3. A strong feature is observed at 635 cm^{-1}, which overlaps with bands observed for hafnia and dysprosium scandate on SiO_2/Si.

Two vibrations are observed at 697 and 615 cm^{-1} for $DyScO_3$/SiO_2/Si and they overlap with a band present for $DyScO_3$ deposited on HfO_2. These bands are absent for Dy_2O_3 as well as for the blank substrate, but close to the peak positions for the Sc_2O_3 film on

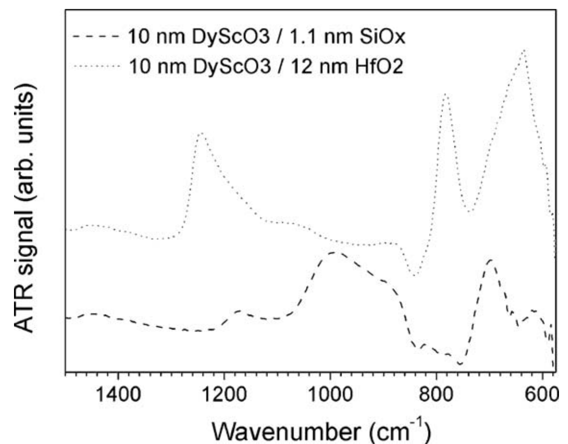

Fig. 5. GATR-FTIR spectra of 10 nm $DyScO_3$ on substrates as indicated.

10 nm SiO_x. Therefore, these features might be typical $DyScO_3$ vibrations, however, they are not derived from theory [38]. The wavenumber is also too high to be ascribed to pure Dy_2O_3 (550 cm^{-1}) or Sc_2O_3 (635 cm^{-1}). However, according to literature, different crystalline lanthanide silicates show bands in the wavenumber region slightly below 700 cm^{-1} [39–41]. Based on the FTIR spectra reported here, Dy_2O_3 does not form this type of silicate but for $DyScO_3$ and Sc_2O_3 it would be a possible explanation for the observations. Furthermore, recently it was reported in Ref. [9] that 12 nm $DyScO_3$/20 nm SiO_2/Si formed silicates after annealing at 1000 °C. A crystalline Sc-rich (Dy,Sc)-silicate was found at the top surface, while at the bottom interface with the substrate an amorphous, Sc-poor Dy-rich silicate was found. These different types of silicate formation may therefore explain the GATR-FTIR observations made here.

3.2.3. Conclusions

GATR-FTIR allows a highly sensitive, inexpensive and fast characterization of ultrathin metal oxide layers with different compositions. Insights in chemical purity, interfacial reactions and crystal phases are obtained, which contribute to the understanding of the high-*k* material's dielectric properties, complementary to more complicated, often destructive analyses.

Interfacial reactions leading to silicate formation, were demonstrated in Dy_2O_3 and $DyScO_3$. A thin SiO_2 interlayer was shown to be entirely consumed by the silicate formation, while deposition of a HfO_2 buffer layer prevented the interfacial reaction. On the other hand HfO_2, $HfScO_x$ and $HfDyO_x$ layers were silicate-free, independent of the substrate's SiO_2 thickness or the anneal treatment.

Finally, GATR-FTIR was shown to be highly sensitive to monoclinic HfO_2, and surpasses deep UV micro-Raman measurement. GATR-FTIR demonstrated that doping hafnia with Dy or Sc, prevents crystallization of the monoclinic hafnia phase. The improved permittivity of the doped films can be ascribed to the formation of the cubic phase.

Acknowledgements

A. Hardy and M.K. Van Bael are postdoctoral research fellows of the Research Foundation Flanders (FWO-Vlaanderen). This study was supported by the FWO research project G.0273.05. The authors thank Dr. R. Lewandowska at Horiba Jobin Yvon, Villeneuve d'Ascq, for the deep UV micro-Raman measurements of HfO_2 films.

References

[1] J. Robertson, High dielectric constant gate oxides for metal oxide Si transistors, Rep. Prog. Phys. 69 (2006) 327–396.
[2] G.D. Wilk, R.M. Wallace, J.M. Anthony, High-kappa gate dielectrics: current status and materials properties considerations, J. Appl. Phys. 89 (2001) 5243–5275.
[3] D. Ceresoli, D. Vanderbilt, Structural and dielectric properties of amorphous ZrO_2 and HfO_2, Phys. Rev. B 74 (2006) 125108.
[4] X.Y. Zhao, D. Vanderbilt, First-principles study of structural, vibrational, and lattice dielectric properties of hafnium oxide, Phys. Rev. B 65 (2002) 233106.
[5] K. Kita, K. Kyuno, A. Toriumi, Permittivity increase of yttrium-doped HfO_2 through structural phase transformation, Appl. Phys. Lett. 86 (2005) 102906.
[6] C. Adelmann, V. Sriramkumar, S. Van Elshocht, P. Lehnen, T. Conard, S. De Gendt, Dielectric properties of dysprosium- and scandium-doped hafnium dioxide thin films, Appl. Phys. Lett. 91 (2007) 162902.
[7] E. Rauwel, C. Dubourdieu, B. Hollander, N. Rochat, F. Ducroquet, M.D. Rossell, G. Van Tendeloo, B. Pelissier, Stabilization of the cubic phase of HfO_2 by Y addition in films grown by metal organic chemical vapor deposition, Appl. Phys. Lett. 89 (2006) 012902.
[8] S. Govindarajan, T.S. Boscke, P. Sivasubramani, P.D. Kirsch, B.H. Lee, H.H. Tseng, R. Jammy, U. Schroder, S. Ramanathan, B.E. Gnade, Higher permittivity rare earth doped HfO_2 for sub-45-nm metal-insulator-semiconductor devices, Appl. Phys. Lett. 91 (2007) 062906.
[9] C. Adelmann, S. Van Elshocht, A. Franquet, T. Conard, O. Richard, H. Bender, P. Lehnen, S. De Gendt, Thermal stability of dysprosium scandate thin films, Appl. Phys. Lett. 92 (2008) 112902.
[10] C. Zhao, T. Witters, B. Brijs, H. Bender, O. Richard, M. Caymax, T. Heeg, J. Schubert, V.V. Afanas'ev, A. Stesmans, D.G. Schlom, Ternary rare-earth metal oxide high-*k* layers on silicon oxide, Appl. Phys. Lett. 86 (2005) 132903.
[11] M.L. Green, M.Y. Ho, B. Busch, G.D. Wilk, T. Sorsch, T. Conard, B. Brijs, W. Vandervorst, P.I. Raisanen, D. Muller, M. Bude, J. Grazul, Nucleation and growth of atomic layer deposited HfO_2 gate dielectric layers on chemical oxide (Si–O–H) and thermal oxide (SiO_2 or Si–O–N) underlayers, J. Appl. Phys. 92 (2002) 7168–7174.
[12] L. Nyns, A. Delabie, M. Caymax, M.M. Heyns, S. Van Elshocht, C. Vinckier, S. De Gendt, HfO_2 atomic layer deposition using $HfCl_4/H_2O$: the first reaction cycle, J. Electrochem. Soc. 155 (2008) G269–G273.
[13] L. Nyns, L. Hall, T. Conard, A. Delabie, W. Deweerd, M. Heyns, S. Van Elshocht, N. Van Hoornick, C. Vinckier, S. De Gendt, Nucleation and growth behavior of atomic layer deposited HfO_2 films on silicon oxide starting surfaces, J. Electrochem. Soc. 153 (2006) F205–F209.
[14] S. Miyazaki, H. Nishimura, M. Fukuda, L. Ley, J. Ristein, Structure and electronic states of ultrathin SiO_2 thermally grown on Si(1 0 0) and Si(1 1 1) surfaces, Appl. Surf. Sci. 114 (1997) 585–589.
[15] N. Rochat, A. Chabli, F. Bertin, M. Olivier, C. Vergnaud, P. Mur, Attenuated total reflection spectroscopy for infrared analysis of thin layers on a semiconductor substrate, J. Appl. Phys. 91 (2002) 5029–5034.
[16] N. Rochat, K. Dabertrand, V. Cosnier, V. Zoll, P. Besson, U. Weber, Infrared spectroscopy of high *k* thin layer by multiple internal reflection and attenuated total reflection, Phys. Stat. Sol. (c) 0 (2003) 2961–2965.
[17] C. Adelmann, P. Lehnen, S. Van Elshocht, C. Zhao, B. Brijs, A. Franquet, T. Conard, M. Roeckerath, J. Schubert, O. Boissière, C. Lohe, S. De Gendt, Growth of dysprosium-, scandium-, and hafnium-based third generation high-dielectrics by atomic vapor deposition, Chem. Vapor Depos. 13 (2007) 567–573.
[18] R. Thomas, P. Ehrhart, M. Roeckerath, S. Van Elshocht, E. Rije, M. Luysberg, M. Boese, J. Schubert, M. Caymax, R. Waser, Liquid injection MOCVD of dysprosium scandate films – deposition characteristics and high-*k* applications, J. Electrochem. Soc. 154 (2007) G147–G154.
[19] M.A. Quevedo-Lopez, J.J. Chambers, M.R. Visokay, A. Shanware, L. Colombo, Thermal stability of hafnium-silicate and plasma-nitrided hafnium silicate films studied by Fourier transform infrared spectroscopy, Appl. Phys. Lett. 87 (2005) 012902.
[20] N. Nagai, H. Hashimoto, FT-IR-ATR study of depth profile of SiO_2 ultra-thin films, Appl. Surf. Sci. 172 (2001) 307–311.
[21] D.P. Zarubin, The two-component bands at about 4500 and 800 cm^{-1} in infrared spectra of hydroxyl-containing silicas. Interpretation in terms of Fermi resonance, J. Non-Cryst. Solids 286 (2001) 80–88.
[22] C. Dubourdieu, H. Roussel, C. Jimenez, M. Audier, J.P. Senateur, S. Lhostis, L. Auvray, F. Ducroquet, B.J. O'Sullivan, P.K. Hurley, S. Rushworth, L. Hubert-Pfalzgraf, Pulsed liquid-injection MOCVD of high-K oxides for advanced semiconductor technologies, Mater. Sci. Eng. B: Solid State Mater. Adv. Technol. 118 (2005) 105–111.
[23] D.A. Neumayer, E. Cartier, Materials characterization of ZrO_2–SiO_2 and HfO_2–SiO_2 binary oxides deposited by chemical solution deposition, J. Appl. Phys. 90 (2001) 1801–1808.
[24] C. Dubourdieu, E. Rauwel, C. Millon, P. Chaudouet, F. Ducroquet, N. Rochat, S. Rushworth, V. Cosnier, Growth by liquid-injection MOCVD and properties of HfO_2 films for microelectronic applications, Chem. Vapor Depos. 12 (2006) 187–192.
[25] D. Dubourdieu, S. Van Elshocht, C. Adelmann, in WoDiM Workshop on Dielectrics in Microelectronics, Bad Saarow (Berlin), 2008, personal communication.
[26] A. Delabie, G. Pourtois, M. Caymax, S. De Gendt, L.A. Ragnarsson, M. Heyns, Y. Fedorenko, J. Swerts, J.W. Maes, Atomic layer deposition of hafnium silicate gate dielectric layers, J. Vac. Sci. Technol. A 25 (2007) 1302–1308.
[27] H. Ono, T. Katsumata, Interfacial reactions between thin rare-earth-metal oxide films and Si substrates, Appl. Phys. Lett. 78 (2001) 1832–1834.
[28] W.L. Baun, N.T. McDevitt, Infrared absorption spectra of rare-earth oxides in the region 800 to 240 cm^{-1}, J. Am. Ceram. Soc. 46 (1963) 294–1294.
[29] N.T. McDevitt, W.L. Baun, Infrared absorption study of metal oxides in the low frequency region (700–240 cm^{-1}), Spectrochim. Acta 20 (1964) 799–808.
[30] N.T. McDevitt, A.D. Davidson, Infrared lattice spectra of cubic rare earth oxides in region 700 to 50 cm^{-1} 56 (1966) 636.
[31] D.B. Faithful, S.M. Johnson, I.J. McColm, Infrared-spectra of lanthanide sesquioxides 10 (1973) 291–302.
[32] H. Vidal, S. Bernal, R.T. Baker, D. Finol, J.A.P. Omil, J.M. Pintado, J.M. Rodriguez-Izquierdo, Characterization of La_2O_3/SiO_2 mixed oxide catalyst supports, J. Catal. 183 (1999) 53–62.
[33] N.B. Colthup, L.H. Daly, S.E. Wiberley, Introduction to Infrared and Raman Spectroscopy, third ed., Academic Press, San Diego, 1990.
[34] S. Jeon, H.S. Hwang, Effect of hygroscopic nature on the electrical characteristics of lanthanide oxides (Pr_2O_3, Sm_2O_3, Gd_2O_3, and Dy_2O_3), J. Appl. Phys. 93 (2003) 6393–6395.
[35] S. Van Elshocht, C. Adelmann, T. Conard, A. Delabie, A. Franquet, L. Nyns, O. Richard, P. Lehnen, J. Swerts, S. De Gendt, Silicate formation and thermal stability of ternary rare earth oxides as high-*k* dielectrics, J. Vac. Sci. Technol. A 26 (2008) 724–730.
[36] W.B. White, V.G. Keramidas, Vibrational-spectra of oxides with C-type rare-earth oxide structure, Spectrochim. Acta A A28 (1972) 501.
[37] S.J. Schneider, J.L. Waring, Phase equilibrium relations in the Sc_2O_3–Ga_2O_3 system, J. Res. Nat. Bur. Stand. A 67A (1963) 19–25.

[38] P. Delugas, V. Fiorentini, A. Filippetti, G. Pourtois, Cation charge anomalies and high-kappa dielectric behavior in DyScO3: ab initio density-functional and self-interaction-corrected calculations, Phys. Rev. B 75 (2007) 115126.
[39] L. Kepinski, M. Maczka, M. Drozd, Formation and characterization of Lu silicate nanoparticles in amorphous SiO_2, J. Alloy. Compd. 443 (2007) 132–142.
[40] L. Kepinski, M. Wolcyrz, M. Drozd, Interfacial reactions and silicate formation in highly dispersed Nd_2O_3–SiO_2 system, Mater. Chem. Phys. 96 (2006) 353–360.
[41] L. Kepinski, W. Mista, J. Okal, M. Drozd, M. Maczka, Interfacial reactions and silicate formation in high surface SiO_2 impregnated with La nitrate, Solid State Sci. 7 (2005) 1300–1311.